THE AMERICAN SOCIETY OF MECHANICAL ENGINEERS
345 E. 47th St., New York, N.Y. 10017

97-GT-522

THE INFLUENCE OF FILM-COOLING ON THE AERODYNAMIC PERFORMANCE OF A TURBINE NOZZLE GUIDE VANE

C. Osnaghi*, A. Perdichizzi**, M. Savini**,
P. Harasgama***, E. Lutum***

* Dipartimento di Energetica, Politecnico di Milano,
Piazza Leonardo da Vinci 32, 20133 Milano, Italy
** Facolta di Ingegneria, Università di Bergamo,
Viale Marconi 5, 24044 Dalmine (BG), Italy
*** ABB Power Generation Ltd., Gas Turbine Development,
5401 Baden, Switzerland

Abstract

The paper presents the results of an investigation on the aerodynamic performance of a full coverage film-cooled nozzle guide vane. The blading is a typical high pressure turbine vane of advanced design, working in the high subsonic regime.

Tests have been carried out for a wide range of conditions, including variations in Mach number, coolant to mainstream mass flow rate ratio and location of the coolant injection. Both air and carbon dioxide at ambient conditions have been utilized, as coolant flow. Measurements have been performed in a plane located at 0.5 axial chord downstream of the trailing edge by means of a miniaturized five-hole pressure probe.

Performances, in terms of losses, flow angles and profile pressure distributions, for different cooling mass flow rates are presented and compared to the results of the solid blade tests (i.e. with no cooling holes). The results showed a significant increase of the losses with blowing . Test with air and carbon dioxide provided almost equal losses if carried out at the same global momentum flux ratio; however the density ratio was found to influence slightly the share of the coolant fluid among the injection rows and the local momentum flux ratio as well.

In order to define the individual contributions of groups of cooling rows on the performance of the blade, three different modes of injection have been tested, namely full, trailing edge and shower head injection. The main trend observed is that trailing edge injection produces the least amount of additional losses at high blowing rates. Full-coverage film-cooling injection did not lead to marked variations in the blade pressure distribution and/or outlet flow angle.

Nomenclature

c = chord
c_p = specific heat at constant pressure
C = concentration
C_D = discharge coefficient
d = diameter
D = density ratio, jet-to-freestream
h = height, enthalpy
I = momentum flux ratio, jet-to-freestream
l = lenght
m = mass flow rate
M = Mach number
MFR = mass flow rate ratio, jet-to-freestream
P = pressure
R = gas constant
Re = Reynolds number
s = pitch
T = temperature
V = velocity
Tu = turbulence intensity
x, y, z = axial, pitchwise and spanwise coordinate
β = flow angle with respect to tangential direction
γ = specific heat ratio
ζ = energy loss coefficient
ρ = density

Presented at the International Gas Turbine & Aeroengine Congress & Exhibition
Orlando, Florida — June 2–June 5, 1997

subscripts

1 = inlet
2 = exit
c = coolant
d = design
ext = external
is = isentropic
mix = mixture
pr = primary
s = static
th = thermodynamic
T = total

Introduction

In advanced gas turbine design, the quest of better performances demands a continuous increase of turbine inlet temperature; to this aim, large efforts are currently done to improve blade cooling techniques. Full coverage of turbine blading by film cooling is one of the most effective ways to sustain higher inlet temperature and it is commonly employed in new engine designs. Two aspects have to be carefully studied: the first one, not discussed in the present paper, is the thermal problem, which requires the knowledge of cooling effectiveness and heat transfer coefficients; the second one is the aerodynamic problem. The coolant injection, in fact, interacts with the mainstream flow and in general produces significant loss penalties.

Several previously published papers investigated this problem on the base of cascade testing; most of them examined the effects of individual injection rows, depending on their position along the blade surface. Ito et al.(1980) reported on the influence of early injection on suction and pressure side at low speed. Kost and Holmes (1985) investigated different trailing edge injection configurations for a transonic rotor blade; they separated the injection loss from the profile loss as a function of coolant flow rate, by considering the base pressure changes. Mee (1990) reported results on experiments at high speed, for trailing edge ejection, with different coolant to mainstream gas density ratios; he found that the losses rise progressively with the coolant flow rate. He also showed that tests at the same momentum flux ratio may be adequate for the loss measurements. Haller and Camus (1984) investigated the effects on the losses of five different injection locations along the suction side, for transonic and supersonic conditions. Surprisingly the injections downstream of the throat did not produce higher losses compared to the upstream ones and no significant loss differences were found for changes in coolant density at constant blowing rates.

Some other papers presented results on multiple row injection configurations: Kiock et al. (1985) investigated three different cooling configurations by means of boundary layer and wake traverses; they have shown the effects of air injection on boundary layer transition and shock configurations. Kollen and Koschel (1985) reported on the individual effects of different row positions in an annular cascade, both at low and high speed. They also compared the measured losses with the results of different loss prediction methods. Yamamoto et al. (1990) analyzed the secondary flow field throughout a linear cascade at low speed for 10 different injection slots along the profile

Due to the great variety of blading geometries, injection configurations, operating conditions and loss definitions, from the above investigations a clear trend of general validity for the loss penalty associated to different injection rates cannot be established. Furthermore, data on blading with complete film cooling, as typical of advanced design, can scarcely be found in the open literature. The present research program has been undertaken to investigate the aerodynamic behavior of a state-of-the-art film cooled high pressure gas turbine vane, for different blowing conditions. The vane was designed for an outlet Mach number $M_{2is} = 0.85$ with a relevant contraction of the channel height. It is characterized by full coverage film cooling with 12 injection rows, by a high blade loading and by a substantial diffusion on the rear suction surface.

The test conditions have been established as closely as as possible to the engine conditions: carbon dioxide was used as coolant flow, to approach the real density ratio between coolant and mainstream flow, a high turbulence level was generated in the incoming flow and finally one of the endwalls was contoured in order to get the correct axial velocity density ratio, as in the real engine. Particular attention has been given to the data reduction and to the loss evaluation, to account for the variations of fluid thermodynamic properties, due to carbon dioxide injection.

Experimental Apparatus

Wind Tunnel

The tests were performed in the transonic wind tunnel for linear cascades of C.N.P.M. (Centro Nazionale per Ricerche sulla Propulsione e l'Energetica, Milano). The tunnel is a blow-down type facility, with a large air storage capacity (3100 kg at 200 bar), permitting relatively long running times. In order to carry out film cooled blade tests, the wind tunnel has been modified to allow for secondary fluid injection.

The system, illustrated in Fig. 1, can feed the blades both with air and carbon dioxide at almost ambient temperature

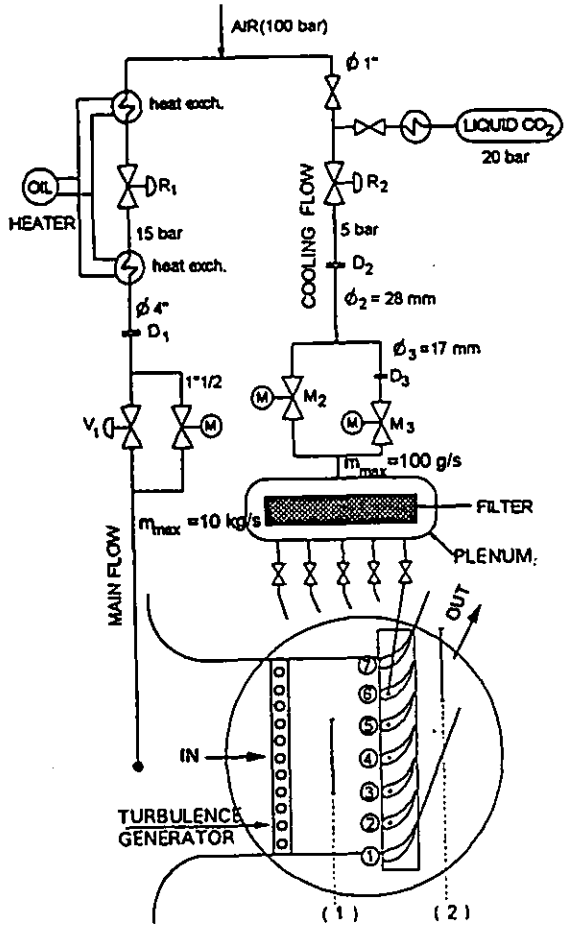

. The CO_2 is supplied by a 2 m^3 tank at 20 bar, where it is stored in liquid phase; the CO_2 piping line is equipped with a pressure reduction valve and an heat exchanger, to assure the complete vaporization of CO_2 (Fig. 1). The main flow feeding system is equipped with a diathermic oil heater, to make possible tests with a temperature difference (50-80 deg. C) between the air of the main flow and the injected fluid; in the present investigation, however, the main flow air was not heated.

After testing devices of different geometries, a turbulence generator consisting of a row of cylindrical bars of diameter $d = 5$ mm and porosity (pitch/diameter) $= 2.0$ has been installed upstream of the cascade (Fig. 1), so as to provide a high level of turbulence intensity (about 7%) at the cascade inlet, approaching the one taking place at the turbine inlet of the real engine.

The total mass flow rate of the coolant, at the nominal (i.e. design) operating conditions in the cascade, is in the range $10 - 100$ g/s, depending on the number of cooled blades and on the blowing rate. In order to characterize each row of holes, down to low discharge velocity, mass flow rate of the order of 0.5 g/s had to be accurately measured. The fulfillment of these requirements was satisfied by using a set of orifices ($4 - 15$ mm diameter) calibrated by means of efficient and miniaturized sonic nozzles.

Cascade Geometry

The cascade consists of 7 blades scaled down to a chord length of 74.5 mm from a first stage nozzle vane. The blade geometry and the cooling holes distribution are qualitatively reported in Fig. 2.

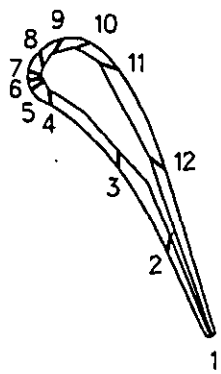

Figure 2: Film cooled nozzle guide vane

The blade row has a relatively high pitch/chord ratio $s/c = 0.861$; this value, that is typical for gas turbine applications, allows to reduce the number of blades and the cooling air flow rate, but it implies that a marked diffusion takes place on the rear part of the suction side. For this reason, in presence of cooling injection, it is important to check if any separation occurs. The holding plate wall has been contoured to reduce the channel height, as in the real nozzle flow passage; the aspect ratio at the exit is $h_2/c = 0.752$.

A unique inner cavity in the film cooled airfoil feeds 11 rows of cylindrical holes distributed along the profile, which assure the full film cooling to the vane. As shown in Fig. 2 there are 3 rows of holes at the leading edge (Shower Head holes), 3 on the pressure side and 5 on the suction side. An additional coolant ejection is performed, through a row of rectangular holes, at the trailing edge. The blowing geometry covered approximately 85 % of the span.

Since the design condition is close to the transonic regime, particular attention has been given to obtaining good periodicity in the downstream flow. To this aim, 5 film cooled blades have been manufactured and set in the central part of

the cascade, so that the four central passages had the same coolant injection. A movable tailboard located at the exit of the first blade allows for the adjustment of the sidewall boundary conditions, to get periodic flow at the cascade outlet.

In order to compare the aerodynamic characteristics in absence of coolant flow, another complete set of solid blades (i.e. without cooling holes) was manufactured and tested. Two adjacent blades have been instrumented, one with 26 holes on the suction side, the other with 21 holes on the pressure side, to get the profile static pressure distribution at midspan. In the cooled vanes, owing to the interaction of the pressure tappings with the cooling channels, some of them were given up, reducing their number respectively to 19 and 15.

Testing Procedure

The tests have been carried out by means of a fully automated computer-controlled data acquisition system. To set the tunnel at the desired testing condition, a procedure has been developed with real time monitoring of the coolant to mainstream mass flow rate ratio (MFR) and of the outlet isentropic Mach number. The cooling flow is measured by an orifice device; the main flow rate is evaluated from the upstream probe data and is based on a reduced blade height to make it consistent with the partial cooling ejection along the span.

The total pressure of the cooling flow is measured in the inner cavity of the blade by a wall pressure tap on the upper plug of the blade, i.e. on the same side of the coolant inlet. A thermocouple fitted on the same plug provides the total temperature of the cooling flow. The flow conditions at the cascade inlet are measured by a wedge type 3 hole probe located at 80% of an axial chord distance upstream of the leading edge. The downstream measurements have been carried out by traversing the flow by a miniaturized 5 hole probe. The measuring plane was located at half an axial chord downstream of the trailing edge. The pitchwise traverses consisted on 46 measuring points, covering 1.4 pitches, while the area measurements consisted on 18 pitchwise traverses at different spanwise positions.

Pitchwise position	$\pm$ 0.1 mm
Spanwise position	$\pm$ 0.1 mm
Flow angle	$\pm$ 0.2 deg.
Stagnation pressure	$\pm$ 0.15% $(p_t - p_s)$
Static pressure	$\pm$ 0.15% $(p_t - p_s)$
Coolant mass flow rate	$\pm$ 1.5%

Table 1: Experimental uncertainties

In the wake traverses the flow was traversed not only at the midspan, but also in 2 more spanwise positions across the midspan, and the profile loss was evaluated by mass averaging the data of these 3 traverses; this, in order to minimize the degree of uncertainty of profile loss. The estimated uncertainties of the measured quantities are given in Table 1.

Loss Evaluation

In testing film cooled blades, it is well known that an important parameter governing the coolant-mainstream flow interaction is the density ratio between the two flows. Also the loss production mechanism is influenced by this parameter, and it is an open question if in fully covered film-cooled blade testing it is necessary to match the real density ratio, to get the correct losses. Matching the experimental conditions to the values typical of real engines is very difficult, and a compromise is needed. To approach such conditions a common practice is to inject carbon dioxide as coolant fluid, but in this case particular attention was given to the data reduction, to avoid errors in the loss evaluation. In the present investigation tests have been performed both with air and carbon dioxide to clarify the differences in the two cases.

The downstream traverse results may be presented in terms of two different energy loss coefficients:

- the Primary loss ζ_{pr}, defined as:

$$\zeta_{pr} = 1 - \frac{V_2^2}{V_{2,is}^2} = \frac{\left(\frac{P_{s2}}{P_{T2}}\right)^{\theta} - \left(\frac{P_{s2}}{P_{T1}}\right)^{\theta}}{1 - \left(\frac{P_{s2}}{P_{T1}}\right)^{\theta}}$$

  where $\theta = (\gamma - 1)/\gamma$.

  By this simplified definition, the contribution of the cooling flow energy is neglected; it means that the ideal kinetic energy of the cooling flow is assumed to be equal to the one of the main flow.

- the so called Thermodynamic loss ζ_{th}:

$$\begin{aligned} \zeta_{th} &= \frac{m(V_{2,is}^2 - V_2^2) + m_c(V_{2c,is}^2 - V_2^2)}{mV_{2,is}^2 + m_c V_{2c,is}^2} \\ &= 1 - \frac{(1 + m_c/m)V_2^2}{V_{2,is}^2 + (m_c/m)V_{2c,is}^2} \end{aligned}$$

  From this definition it results:

$$\zeta_{th} = 1 - \frac{(1 + \frac{m_c}{m})h_{T2mix}\left[1 - \left(\frac{P_{s2}}{P_{T2}}\right)^{\theta_{mix}}\right]}{h_{T1}\left[1 - \left(\frac{P_{s2}}{P_{T1}}\right)^{\theta}\right] + \frac{m_c}{m}h_{Tc}\left[1 - \left(\frac{P_{s2}}{P_{Tc}}\right)^{\theta_c}\right]}$$

This definition takes into account the energy actually introduced into the flow field hy the injection of the cooling flow; therefore this is the loss coefficient to be considered if one wants to establish the actual energy decay in the whole blade system, including the feeding loss in the cooling holes, the mixing loss due to the injection and the profile loss.

The thermodynamic loss coefficient ζ_{th} will be considered as more significant in the result analysis.To determine ζ_{th}, in case of CO_2 injection, the actual thermodynamic properties, R and γ of the air/coolant mixture and T_{t2mix} in the downstream measuring points have to be known. Also for the 5 hole probe data reduction procedure, such data are needed to link the Mach number to the calibration data. To evaluate these quantities, additional traverses of CO_2 concentration and total temperature should be performed for each test, but this would require such long times that are absolutely incompatible with the blow-down wind tunnel running times. To overcome this problem, a procedure has been introduced in the data reduction, which allows to estimate approximately in each measuring point R, γ and T_{t2}. This procedure is based on the assumption that the distribution of carbon dioxide concentration C along the traverse is consistent with the one of total pressure loss, i.e.

$$\frac{C(y)}{C_{\max}} = \frac{(p_{t1} - p_{t2}(y))}{(p_{t1} - p_{t2})_{\max}}$$

This means to assume an analogy between coolant mass diffusion and momentum diffusion, supposing that the diffusion mechanism is mainly due to the turbulence (Schmidt number $\cong$1).

The peak value of the coolant concentration $C_{\max}$ is determined in an iterative way, so that the coolant flow rate, obtained by integrating the coolant mass flow rate throughout the passage, is equal to the value measured by the orifice. This procedure can be used not only in the case of CO_2 injection, but also in the case of air injection with total temperature different from the one of the main flow, to estimate the total temperature of the mixture T_{t2mix}. In this case the assumption is that thermal diffusion is mainly due to turbulent mixing (Lewis number$\cong$1), and that the heat transfer between the coolant and main flow through the blade wall is negligible.

In order to check the validity of the above assumption, the CO_2 concentration for the design injection condition was measured by means of a infrared analyzer. The results of Fig. 3 show a larger extent of the concentration wake on the suction side, that is likely to be due to the larger coolant flow rate blown from the suction side, compared to the one from the pressure side. This result is not in agreement with the assumption made, so a sensitivity analysis was carried out,

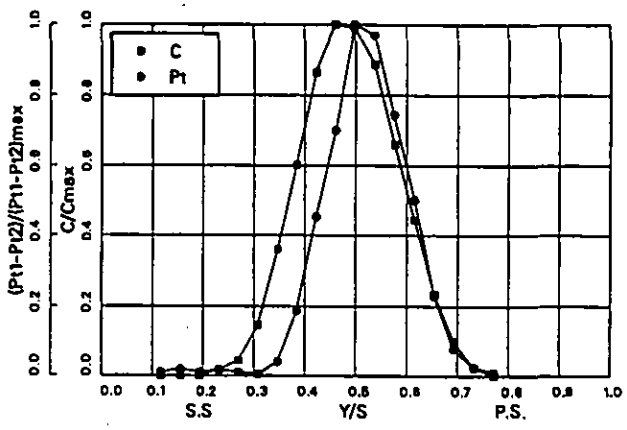

Figure 3: Concentration and total pressure wakes

by considering different concentration distributions: symmetric and asymmetric distribution with respect to the total pressure wake, and uniform distribution along the pitch. It resulted that the local loss coefficient is affected from the assumed distribution, but the pitchwise mass averaged loss variation is not significant ($\Delta\varsigma_{\max} = 0.0002$ for the uniform distribution). On the other hand, appreciable variations take place if the overall coolant flow rate from the concentration data does not correspond to the actually injected flow ($\Delta\varsigma\cong$0.002 for $\mp$20% error in flow rate).

Discharge Coefficients and Coolant Flow Evaluation

The discharge coefficient, defined as $C_D = \frac{\rho V}{(\rho V)_{is}}$, depends, for a given geometry, on the isentropic Mach number M_{is} and Reynolds number Re_{is}, the latter based on the hole diameter. In order to get a reasonable estimate of the influence of the Reynolds number, a set of preliminary tests were conducted on perforated plates with holes of different diameter. It is very difficult to separate in the experiments the effects of the Mach number and Reynolds number, so we prefer to write the relation obtained via this set of tests in the form:

$$C_D = C_D^*(M_{is}) f\left(\frac{Re}{Re^*}\right)$$

where the star refers to a given test condition ($d, l/d$ and kinematic viscosity ν) and C_D^* is, strictly speaking, $C_D^*\left(M_{is}, Re^*\left(M_{is}\right)\right)$. In the range of interest from incompressible to choked flow, the following function gave the best fit

$$f = \left(\frac{Re}{Re^*}\right)^{0.04}$$

By means of this function one can correct the experimental C_D^* data base, in order to take into account the scale effects and the effects of viscosity and density differences between the calibration and the wind tunnel or real gas turbine application. By changing the inner blade pressure, with the outlet pressure fixed (atmospheric), we obtained the curves of Fig. 4 for the 12 rows of holes. The trend of

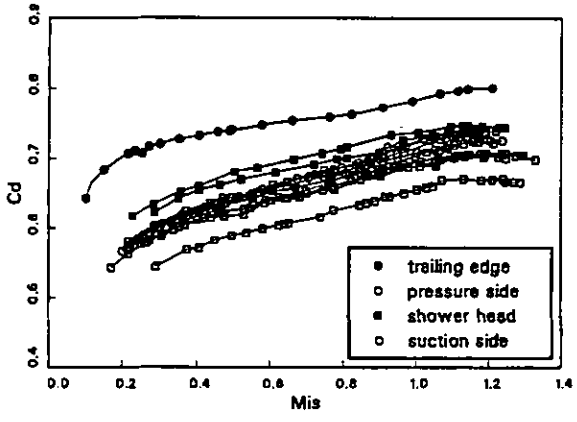

Figure 4: Discharge coefficients

the curves is quite similar and congruent with the l/d ratio, except for the trailing edge holes which have a different shape and an higher hydraulic diameter.

Owing to the small dimensions involved, great attention was devoted to minimize the leakage and the errors in the evaluation of the hole diameter. A further delicate point was the definition of a reference total pressure, because in the blade cavity the velocity is not negligible when all the rows of holes are open. A correction was applied in this case to the inlet total pressure; it was determined from tests with no external flow, so that the sum of coolant flow rates over all the rows (evaluated from the discharge coefficients) corresponds to the global value measured by the orifice device.

Coolant Mass Flow Rate Measurement

The coolant flow rate was measured, for each row of holes, in the wind tunnel with external flow at nominal conditions ($M_{2is} = 0.85$). By comparing the profile blade pressures of the solid blade to the ones of the cooled blade, little differences were found, due essentially to the growth of the main flow rate along the blade due to the coolant injection. The difference is not negligible for the base pressure downstream of the trailing edge.

For each row, it is possible to define an "effective pressure" (to be used in the calculation of the theoretical mass flow rate of the hole), for which the behavior of the discharge coefficient vs. M_{is} is almost the same as the standard one, i.e. the one obtained with no external flow (Fig. 4). This can be verified, as at low mass flow rates the curves of the discharge coefficient are very sensitive to little changes in the assumed external pressure. This "effective pressure" was found to be very close to the true external pressure at the hole discharge (obtained by interpolating the values of the nearest pressure tappings), meaning that the external cross-flow has a negligible influence on C_D ; therefore one can use the discharge coefficients evaluated in absence of external flow. As an example, Fig. 5 shows the situation for row n. 12 , where the "effective pressure" ($M_{is} = 0.950$) corresponds to the experimental value in presence of cooling ($M_{is} = 0.953$).

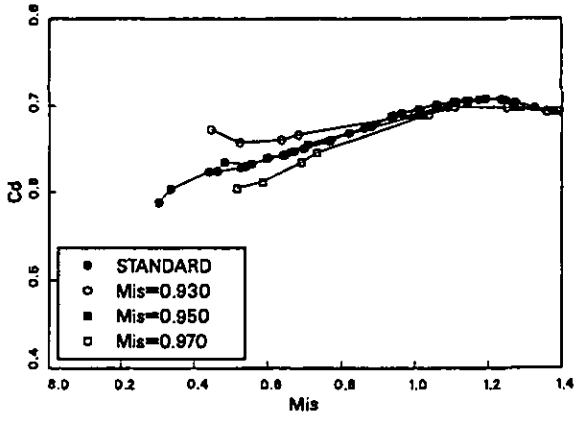

Figure 5: Discharge coefficient for hole n.12 for different assumed exit pressures

Coolant Mass Flow Rate Calculation and Evaluation of Mixing

An automatic computation procedure has been developed to evaluate the cooling exit conditions (velocity and density) of each row of holes, starting from the cooling total conditions, the profile pressure measurements and the hole discharge coefficients. By this procedure it is possible to compute the distribution of the coolant between rows of holes, so one can check the accuracy of the measurements by comparing the injected flow rate to the sum of the flow rates of all the rows.

Starting from the local velocities and densities , two models, based on the assumption of a constant pressure or constant area mixing between the coolant and the main flow, were developed to estimate the local mixing energy losses; the two models gave similar results in our case. The possibility of calculating the individual and global mass flow

rate and mixing loss is interesting for predicting situations with coolant conditions other than the experimentally feasible ones, in particular at realistic temperatures; for instance the results reported in Table 2 (the mixing loss coefficient is the sum of the local mixing losses referred to the vane outlet isentropic conditions) suggest that the use of CO_2 instead of air at very low temperatures is well-founded.

	Mixing Loss Coefficient ζ_{th}		
MFR/MFR_d	Air 15 C	CO_2 15 C	Air -130 C
0.75	0.87%	0.90%	0.95%
1.00	1.72%	1.15%	1.26%
1.25	2.74%	1.68%	1.71%

Table 2: Computed loss based on mixing model

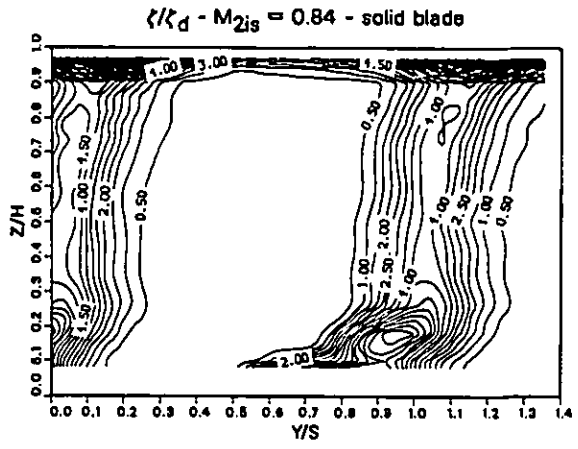

Figure 6: Loss contours

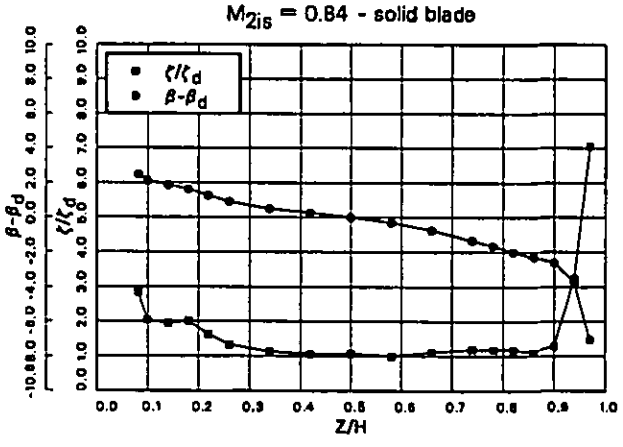

Figure 7: Spanwise loss and angle distributions

Solid Blade Results

Due to the low cascade aspect ratio and the large s/c, the downstream flow is characterized by important 3D effects. Also the presence of the endwall contouring contributes to make even more complex the downstream flow structure. To clarify the flow field configuration, in the case of solid blade cascade, a complete traversing of the measuring plane has been done, for the nominal conditions, i.e. for $M_{2is} = 0.85$.

The results plotted in terms of the local energy loss coefficient (ζ) are shown in Fig. 6, where $z/h = 1.0$ corresponds to the contoured wall, and $z/h = 0.0$ to the flat one.The spanwise distributions of pitchwise averaged losses and outlet flow angle are presented in Fig. 7. Flow angles are presented as deviations from the design value, whilst losses as ratios to the design value; both design values are the pitchwise mass-averaged measured ones for the solid blade at midspan. The loss distribution appears to be significantly influenced by the presence of the contouring. On the flat side, it can be noted the typical secondary flow loss distribution, with a wide core on the wake suction side. On the opposite, at the contoured endwall no trace of this core is present, and the low energy fluid from the inlet boundary layer is squeezed against the wall. The extension of the secondary flow effects from the wall is smaller (from $z/h = 0.85$ to 1.0), if compared to the one on the flat side (from $z/h = 0.0$ to 0.35), and less secondary loss is produced. For a large extent of the channel height, the flow field appears to be practically 2D with a well defined 2D wake. Therefore the profile loss of the vane can be evaluated by pitchwise traversing the flow at midspan.

These results show that the presence of the contouring inhibits the secondary flow development. The explanation for this finding is likely to be the following: the streamtube at the contoured wall undergoes a larger contraction if compared to the one at the flat side, so at the cascade inlet smaller velocities take place, producing a smaller blade loading in the first part of the blade channel, that is just where the flow turning occurs and the passage vortex is forming. As a consequence, the driving force between pressure and suction side is reduced and the passage vortex intensity thus lowered. Then, due to the larger axial velocity density ratio taking place on the contoured side, the high loss region results to be more confined close to the endwall. An additional effect contributing to this phenomenon is the spanwise pressure gradient (directed toward the flat wall) downstream of the throat, caused by the streamline

curvature.

The presence of the contouring influences also the outlet flow angle distribution (Fig. 7) that does not present, indeed, the typical underturning and overturning regions. If the midspan is assumed as reference location, the angle distribution towards the contoured side presents a continuous decrease down to very low values close to the wall. Conversely, towards the flat side the flow angle increases, producing a significant underturning for most of the blade height. This is a consequence of the non uniform pressure distribution along the span at the throat, where the flow angle is nearly constant, the lower pressure being at the contoured side. Moving downstream, the trend towards uniform static pressure forces a relative deceleration at the contoured side, thereby turning the flow in the tangential direction; the opposite, of course, occurs at the flat side.

Film Cooling Test Conditions

The film cooling tests have been performed by traversing the downstream flow at midspan, both with air and CO_2 as coolant flow, for the following conditions:

- $M_{2is} = 0.85$, $MFR \cong 0.6 - 1.4\ MFR_d$
- $MFR = MFR_d$, $M_{2is} \cong 0.7, 0.85, 0.96$.

The above tests have been performed for 3 ejection conditions:

- All rows of holes open.
- Trailing edge ejection only, with all the others rows closed.
- Shower Head ejection only (3 rows open), with all the others closed.

Results with All Holes Open

Tests for Different Mass Flow Rates

The wake traverses results for the nominal expansion ratio and different blowing conditions are presented in Figg. 8-11. These traverses refer respectively to solid blades, film cooled blades with no blowing ($MFR = 0$), carbon dioxide injection with design mass flow rate ratio MFR_d and 1.28 MFR_d. It can be observed that a satisfactory periodicity of the downstream flow has been obtained for all the test conditions. All the tests at different MFR were run at the same expansion ratio, with no restaggering of the vane, so a variation of the blade loading and the outlet flow angle might be expected, due to non-viscous displacement effects induced by the presence of coolant flow.

MFR/MFR_d	0.56	0.72	0.83	1.00	1.11	1.28
$\beta - \beta_d$	0.1	0.1	0.1	0.2	0.2	0.2

Table 3: Outlet flow angle for different MFR

From these results it is evident that the distributions of Mach number and flow angle are weakly influenced by the conditions of coolant ejection; even the pitchwise mass-averaged outlet angle (Table 3) does not present any significant variation with MFR. On the contrary there is a marked influence on the loss distribution: the width of the wake is not influenced by the injection mass flow ratio but the peak value of ζ_{th} in the wake increases significantly with MFR. This occurs as the effect of both the internal hole friction and the increase of coolant mass flow rate overwhelm the reduction in the velocity deficit of the injected flow in the mixing process. In fact the hole internal losses increase both with MFR and coolant velocity, whilst the mixing loss is proportional to MFR times the velocity deficit. For the no blowing case (Fig. 9), one can notice an appreciable increase of the losses with respect to the solid blade. This is caused by the superposition of two effects: one is the well-known fact, e.g. Ito et al. (1980) and Arts (1992), that the presence of the holes may both trigger the transition of the boundary layer and increase the turbulence of a turbulent boundary layer; the other is due to the fraction of the mainstream entering the hollow cavity in the leading edge region and exiting from the suction side and from the trailing edge holes, thus experiencing an additional dissipation. In order to separate these two effects the holes should be sealed from the inside; however, this was not done in the course of the present work.

The "primary losses" ζ_{pr} are also reported in the figures; ζ_{pr} is greater than ζ_{th}, as the CO_2 isentropic outlet velocity at the exit of the cooling holes is substantially lower than the mainstream velocity, this difference decreasing with an increase in MFR. It is interesting to point out that using air as coolant at the same blowing conditions the behavior would be reversed (i.e. ζ_{pr} lower than ζ_{th}), illustrating once again the potentially misleading use of the "primary" losses.

The analysis of the relative share of coolant between the different rows, based on the procedure previously mentioned, showed significant changes with blowing variations. For $MFR = 0.72\ MFR_d$, at the leading edge, there is no cooling flow and the primary flow enters into the vane; in this case most of the flow goes out from the trailing edge (53 %). For $MFR = 1.28\ MFR_d$, there is a flow rate share of about 4% for each row in the front part of the blade, while at the trailing edge it reduces at 33% of the total.

In Fig. 12 are plotted the pitchwise mass-averaged losses

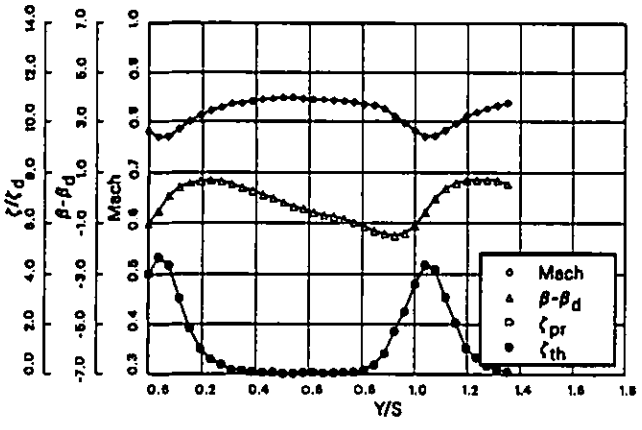

Figure 8: Downstream traverse-solid blade

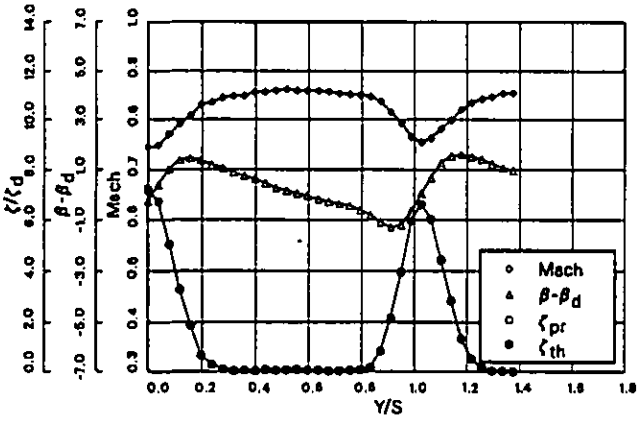

Figure 9: Downstream traverse-$MFR = 0$

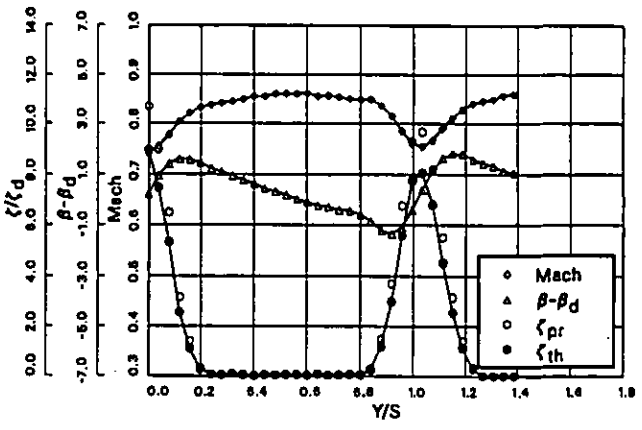

Figure 10: Downstream traverse- $MFR = MFR_d$

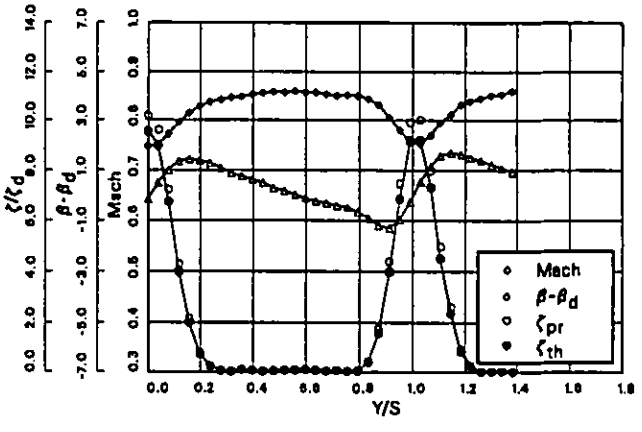

Figure 11: Downstream traverse-$MFR = 1.28MFR_d$

as a function of the coolant mass flow rate for both CO_2 and air. The marked difference between ζ_{th} and ζ_{pr} for both refrigerants gives the error made by neglecting the energy of the injected fluid in the loss definition.

For small values of injection rates the loss variation with respect to the solid blade remains modest, but well below the design point, the losses start to increase significantly exhibiting an increment up to 85% for carbon dioxide and 120% for air at the edge of the investigated range ($MFR = 1.40\ MFR_d$). The bigger loss in case of air injection is mainly due to the higher coolant jet velocities, which cause higher dissipations inside the internal hole passages. This is clearly shown in Fig.13 where global losses are compared to external losses (i.e. global minus internal) both for air and CO_2 tests. The internal losses were computed by mass averaging the internal loss of every row, being the share of coolant between the rows and the loss of each single row evaluated on the basis of the discharge coefficients.

This comparison between air and carbon dioxide is done at fixed mass flow rates, i.e. at fixed blowing rates, but if one compares the losses for air and CO_2 at equal momentum fluxes, thereby comparing the air blowing rate with the CO_2 blowing rate divided with the square root of the density ratio between CO_2 and air, the global losses are much closer one to the other (see Fig. 14). This suggest that the most important parameter governing the aerodynamic losses is the momentum flux ratio. This result, that is in agreement with the one of Mee (1992) obtained for single trailing edge ejection, in this case with multiple row injection, where a change in density ratio (at equal global momentum flux ra-

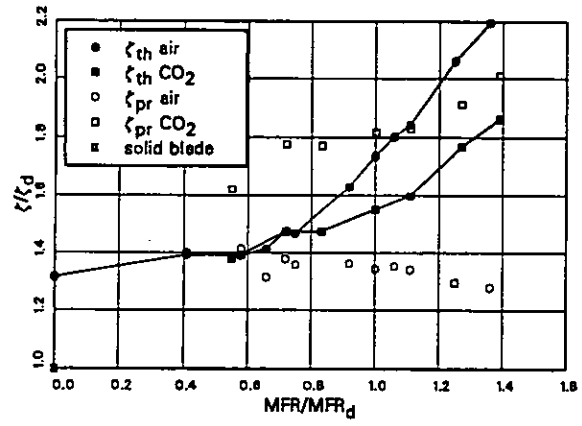

Figure 12: Losses vs. coolant mass flow rate

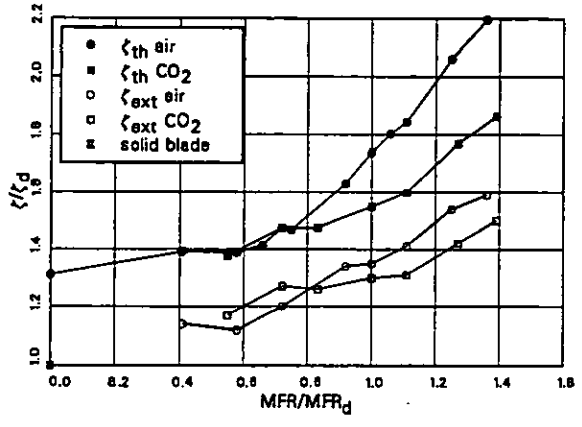

Figure 13: Global and external losses vs MFR

tio) implies a change in the relative share of coolant among the rows, is surprising. It is authors' opinion that this is not a result of general validity.

This result is to be related to the fact that internal losses are the dominant factor in the loss increase due to coolant injection. In fact, if one considers this loss alone and supposes laminar flow inside the cooling holes, so that the friction coefficient is inversely proportional to the coolant velocity, one can conclude that the loss coefficient depends only on the momentum flux ratio. However situations where internal losses are dominant are not likely to be the rule; in this case we are dealing with low discharge coefficients (due to the sharp hole inlet and to probable crossflow in the vane cavity); on the other hand this is a well designed film-cooled airfoil, so that mixing and cooling-induced boundary layer losses are very low.

The work of Pietrzyk et al. (1990) showed that the details

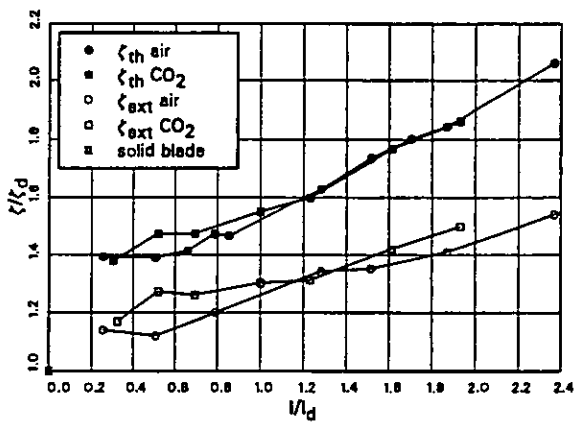

Figure 14: Losses vs. momentum flux

of the mixing process downstream of the injection holes are influenced by the density ratio; this may be important in cases where local boundary layer effects are significant.

Therefore the conclusion that naturally stems from the above discussion is that it is advisable to use in the experiment a density ratio as close as possible to the actual value of the real machine.

Tests at Different M_{2is}

The variation of the profile Mach number blade distribution caused by the film-cooling at MFR_d is shown in Fig. 15. As one can see the coolant injection does not alter significantly the pressure on the profile for the whole range of expansion ratios considered. Apart from a small over-acceleration at the exit of each cooling hole, higher velocities on the blade suction side downstream of the throat are noticeable. These are a consequence of the additional mass flow provided by the coolant. It is worth to mention that at nominal M_{2is} the injection does not impair the pressure recovery in the rear part of the blade, as could happen in a highly loaded cascade.

For $M_{2is} = 0.955$ larger velocities take place on the suction side beyond $x/c = .35$, and the shock wave moves towards the trailing edge; as expected, larger differences take place in the high velocity region where even small cooling injection cause significant velocity variations.

Increasing the Mach number, small variations of the sharing of the mass flow rate among the injection rows take place. Only a decrease of about 1-2% of the trailing edge ejection, for a variation of M_{2is} from 0.7 to 0.955 has been found.

The Thermodynamic loss ζ_{th}, vs. M_{2is}, for the design mass flow rate ratio is reported in Fig. 16. The trend is

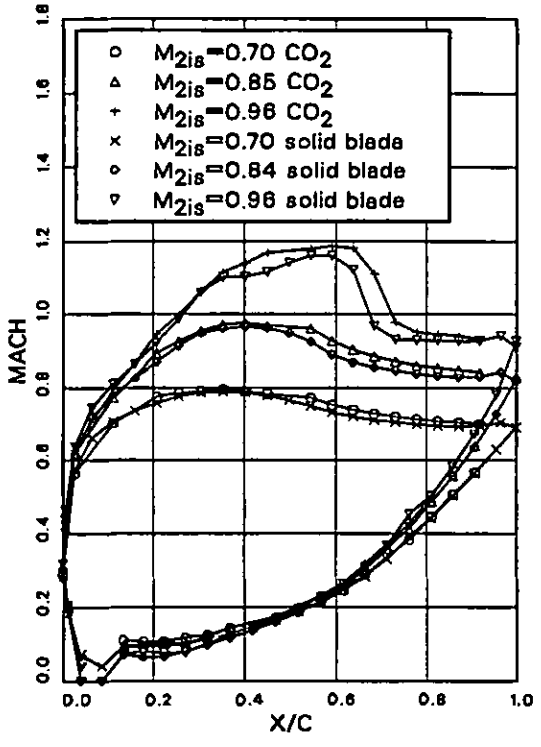

Figure 15: Profile isentropic Mach number

similar to the one obtained for the solid blade, but the loss is significantly higher because of internal aerodynamic loss and film cooling mixing as well; this stands both for the CO_2 and air tests. As the curves resemble the solid blade ones, it can be concluded that for the present blade the coolant injection does not change dramatically the aerodynamic characteristics, even in the transonic range at off-design expansion ratios.

Results with Partial Filming

In order to quantify the individual contribution of different rows of holes to the losses, tests have been performed with partial blockage of the cooling holes. Here are presented and discussed results obtained for the T.E. row injection (all the other rows closed) and for the Shower Head injection (only the leading edge rows open), in case of carbon dioxide. The tests with partial filming have been done by blocking the remaining holes by a thin aluminium tape (0.1 mm thickness), so to cover the vane part not affected by the film cooling.

Exit traverses were performed for the same operating conditions as in the full injection tests, i.e.:

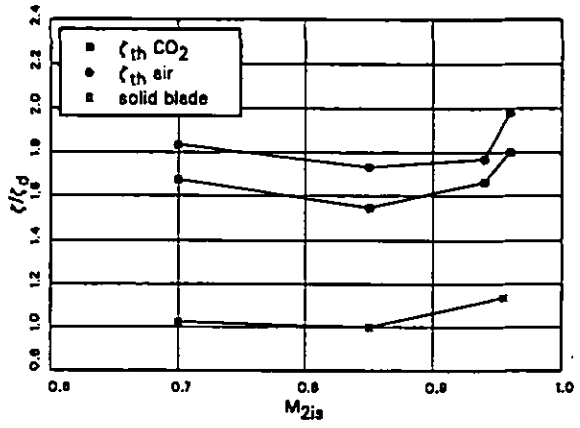

Figure 16: Losses vs. M_{2is}at MFR_d

- $M_{2is} = 0.85$, $MFR \cong 0.6 - 1.38\ MFR_d$
- $MFR = MFR_d$, $M_{2is} \cong 0.7, 0.85, 0.96$.

It has to be pointed out that, for each test condition, a flow rate has been injected, equal to the one blown from the rows under consideration as in the case of full injection. Such flow rate has been estimated by sharing the injected flow between all the rows, on the basis of the discharge coefficients. Therefore, the MFR considered in the partial filming tests is the overall MFR, and not the ratio between the flow rate actually injected and the main flow rate. By using this MFR definition it is possible to draw the results of full and partial injection on the same plot, so as to compare the effects of the different blowing locations on the loss production.

Tests for Different Mass Flow Rates

The results of the tests for different blowing rates are presented in terms of pitchwise mass-averaged loss ζ_{th}., in Fig. 17. One can see that for the nominal MFR, the Shower Head injection is responsible for about 20% of the total loss increase, whilst the Trailing Edge one contributes for about 50 % ; hence, all the other rows produce the remaining 30% of the losses. If one considers that the estimate share of the injected flow rate is 8% for the S.H., 38% for the T.E. and 54% for all the other rows, it comes out that the injection at the leading edge is more critical, as small injection rates produce a relatively large loss increase. On the opposite the injection through pressure and suction side rows result to he much less penalizing for the cascade aerodynamics. By comparing the loss traverses (not presented here) for the S.H. ejection to the corresponding ones of the T. E. ejection, it has been noted that for the S.H. injection, the loss

peak value is much smaller, but the wake width is greater, originating from a thicker boundary layer at the exit of the bladed channel.

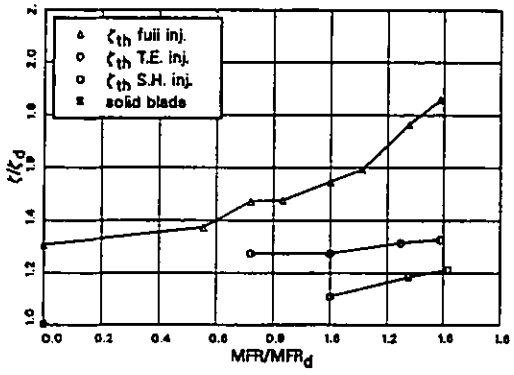

Figure 17: Losses vs. $MFR_d$for different injection modes

Increasing the MFR above the design value, the slope of loss increase relative to the T.E. contribution is the smallest one, thus indicating that large T.E. injections are potentially less dangerous for the cascade efficiency. In fact, it has already been found by many authors (Kiock et al. (1985), Kost and Holmes (1985), Sieverding (1982)) that a small injection rate in the base region is beneficial for the losses, as it energizes the wake flow and increases the base pressure thereby reducing the base pressure loss. Conversely high injection rates imply larger penalties for the S.H. and for all the remaining rows as well.

For the tests below the design condition, i.e. at $MFR = 0.72\ MFR_d$; the loss share due to trailing edge injection rises up to about 60% of the total; this because the fraction of coolant flow rate injected at the trailing edge increases significantly and hence higher losses take place; for this condition in fact, the coolant flow rate at the leading edge becomes negative (i.e. mainstream flow entering the blade), and this is the reason why points for S.H. injection are not drawn in the plot.

Tests for Different M_{2is}

Fig. 18 provides a comparison of the loss coefficients vs. M_{2is}, for the three injection modes at the design MRF. For the S.H. ejection the trend is similar to the one obtained for the solid blade, with a greater loss occurring at $M_{2is} = 0.7$.

For the T.E. ejection the mass averaged losses appear to be not much influenced by the Mach number; there is a slight decrease in the range from $M_{2is} = 0.7$ up to 0.85, as in the full injection tests, but for $M_{2is} = 0.95$, no significant loss increase have been found.

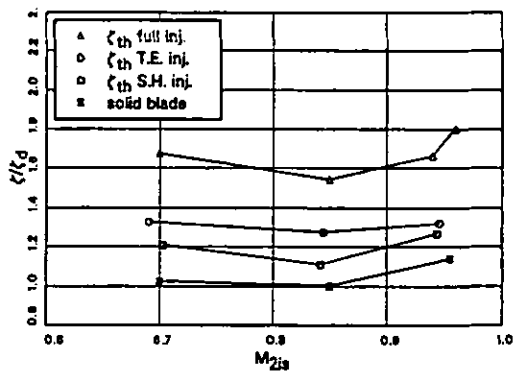

Figure 18: Losses vs M_{2is}at$MFR_d$for different injection modes

Conclusions

The present investigation on the aerodynamic influence of film cooling for a nozzle guide vane, representative of high pressure nozzles of advanced design, allowed to reach the following conclusions:

- The loss penalty due to film-cooling increases with blowing; at the design condition it is quite significant, being about 50% of the solid blade loss. An important role in the loss increase is played by internal aerodynamic losses. No variation of the outlet flow angle due to coolant injection was observed.
- Higher losses take place in case of air injection, with respect to carbon dioxide, but if tests are performed at the same global momentum flux ratio, almost equal mass averaged losses were found. However the density ratio has a non negligible impact on the flow rate share among the injection rows.
- By using carbon dioxide as refrigerant fluid, a proper data reduction has to be employed to take into account the local properties of the mixture which depend on the local coolant concentration. A simple and effective way to perform this task was shown here.
- The use of ζ_{th} as energy loss coefficient is to be preferred as ζ_{pr} is misleading.
- Even small injection rates through Shower Head holes cause significant loss penalties. Relatively lower losses, if compared to the flow rate share, are generated by the injections on the pressure and suction surfaces. With increasing the coolant flow rate the loss penalty due to trailing edge ejection remains almost constant, whilst all the others undergo a significant rise.

- The profile Mach number distribution is not much influenced by coolant injection. Only on the rear suction side appreciably higher velocities have been found. The required amount of film cooling was injected, without flow separation in the diffusing rear suction surface.

Acknowledgments

The authors wish to thank ABB Power Generation Ltd. for their support and permission to publish this paper.

References

Arts,T., Lapidus, I.., 1992, "Thermal Effects of a Coolant Film along the Suction Side of a High Pressure Turbine Nozzle Guide Vane", AGARD CP 527 "Heat Transfer and Cooling in Gas Turbines", Antalya (Turkey), September 1992.

Hay, N., Lampard, D., 1996, "Discharge Coefficients of Turbine Cooling Holes: A Review", ASME paper 96-GT-492.

Haller, B.R., Camus, J.J., 1984, "Aerodynamic Loss Penalty Produced by Film-Cooling Transonic Turbine Blades", ASME Journal of Engineering for Gas Turbines and Power, Vol.106, pp.198-205.

Ito, S., Eckert, E.R., Goldstein, R.J., 1980, "Aerodynamic Loss in a Gas Turbine Stage with Film-Cooling", ASME Journal of Engineering for Power, Vol.102, pp.964-970.

Kiock,R., Hoheisel, H., Dietrichs, H.J., Holmes, A.T., 1985, "The Boundary Layer Behaviour of an Advanced Gas Turbine Rotor Blade under the Influence of Simulated Film-Cooling", AGARD CP 390 "Heat Transfer and Cooling in Gas Turbines", Bergen (Norway), May 1985.

Koellen, O., Koschel, W., 1985, "Effect of Film-Cooling on the Aerodynamic Performance of a Turbine Cascade", AGARD CP 390 "Heat Transfer and Cooling in Gas Turbines", Bergen (Norway), May 1985.

Kost, F.H., Holmes, A.T., 1985, "Aerodynamic Effect of Coolant Ejection in the Rear Part of Transonic Rotor Blades", AGARD CP 390 "Heat Transfer and Cooling in Gas Turbines", Bergen (Norway), May 1985.

Mee, D.J., 1992, "Techniques for Aerodynamic Loss Measurement of Transonic Turbine Cascades with Trailing-Edge Region Coolan Ejection", ASME paper 92-GT-157.

Pietrzyk, J.R., Bogard, D.G., Crawford, M.E., 1990, "-Effects of Density Ratio on the Hydrodynamics of Film-Cooling", ASME Journal of Turbomachinery, Vol.112, pp. 437-443.

Sieverding, C.H., 1982, "The Influence of Trailing-Edge Ejection on the Base Pressure in Transonic Turbine Cascades", ASME paper 82-GT-50.

Thole, K., Gritsch, M., Schultz, A., Wittig, S., 1996, "Flowfield Measurements for Film Cooling Holes with Expanded Exits", ASME paper 96-GT-174.

Yamamoto, A., Kondo, Y., Murao, R., 1990, "Cooling Air Injection into Secondary Flow and Loss Fields Within a Linear Turbine Cascade", ASME paper 90-GT-141.